

Experimental Research on Heat/Mass Transfer Features of Corrugated Plate Spray Humidification Air Coolers

Xiaoqing Huang^{*a,b}, Dongliang Zhang^a, Xu Zhang^c

^aCollege of Energy and Power Engineering, Nanjing Institute of Technology, Nanjing 211167, China

^bSchool of Energy and Environment, Southeast University, Nanjing 210096, China

^cInstitute of HVAC & Gas, Tongji University, Shanghai 201804, China

hxq-101@163.com

This paper studies the heat/mass transfer features of a brand-new air cooling device, the corrugated plate spray humidification air cooler, under dry and wet working conditions. Specifically, the author compared the air and water cooling effects of the same nozzle type in different layouts and different nozzle types in the same layout. The TF6 nozzle type + 500mm×500mm layout was confirmed as the optimal working conditions for the heat exchanger under wet conditions. The results show that the spray increased both the logarithmic mean temperature difference (LMTD) of the heat exchanger and the air-side heat transfer coefficient, without obstructing the air-side flow or adding to the air resistance. Moreover, the relationship between the contact coefficient, air mass velocity and water-air ratio was obtained through data fitting.

1. Introduction

Air cooling is one of the most effective water-saving measures in power stations. However, the cooling effect is heavily influenced by the ambient temperature. Under the high ambient temperature in summer, the hot fluid outlet temperature of the air cooler cannot meet the process requirements. To solve this problem, evaporative cooling has been proposed to promote the air side heat transfer of the air cooler. The typical applications include hybrid (dry/wet) air cooler, deluge-type air cooler and (packing/spray) humidification air cooler. Among them, the spray humidification air cooler cools down the inlet air by spraying water vapour through a nozzle. Because of low initial investment, high rate of return and relatively simple system, the spray humidification air cooler was selected as the object of this research (Xuan et al., 2007; Duan et al., 1998).

Since the air has a small heat transfer coefficient, the key aims of an air cooler are enhancing heat transfer, reducing flow resistance and increasing compactness. Therefore, the corrugated plate heat exchanger, known for efficient heat exchange and compact structure, enjoys bright market prospects. In this paper, several experiments are carried out on a corrugated plate spray humidification air cooler. The cooler is a brand-new air cooling device with a structure entirely different from that of traditional tubular air cooler or finned tube air cooler.

Over the years, Kachhwaha, Stoitchkov, Armbruster, Yan, Wang, Kim, Cherif, Bell, Heyns and others (Kachhwaha et al., 1998; Stoitchkov and Dimitrov, 1998; Armbruster and Mitrovic, 1998; Yan, 1998; Wang and Mamishev, 2012; Kim et al., 2011; Cherif et al., 2011; Bell et al., 2011) have all contributed to the research on the heat/mass transfer and flow resistance features of evaporative coolers. In terms of the heat/mass transfer coefficient, the mass transfer coefficient is usually obtained through experiment, and the heat transfer coefficient through analogy using the Lewis relationship equation.

2. Experimental System and Working Conditions

The experimental system comprises a humidification system, a hot fluid system, an air system and a measurement control system. The humidification system and a corrugated plate heat exchanger (Figure 1) form the experimental section. In the heat exchanger, there are two rows of nozzles, each of which has two nozzles. The nozzles are arranged in three different layouts: (L×W) 500mm×500mm, 500mm×725mm, and

725mm×725mm. The hot fluids flow into the heat exchanger from the top right corner and flows out from the top left corner.

Under dry working conditions, the air cools down the hot fluid directly from outside of the plate bundle. Both the air and the hot fluid are subject to cross-flow heat exchange. Under wet working conditions, the nozzles on the side of plate bundle open up and eject fluid at the air inlet. Figure 2 illustrates the structure of the experimental section of the heat exchanger. The hot fluid flows in the plate bundle through a 6.4mm-wide channel, and the air flows outside the plate bundle also through a 6.4mm-wide channel. The 0.7mm-thick corrugated plate is made of stainless steel. The spiral pressure nozzle TF4 and air atomizing nozzle AM4 (Figure 3) were selected for the experiments.

The experiments were conducted under both dry and wet working conditions. The dry conditions include variable air volumes (VAV) and variable water volumes (VWV). In addition to the VAV and the VWV, the wet conditions also involve different layouts of the same nozzle type, and different nozzle types in the same layout.

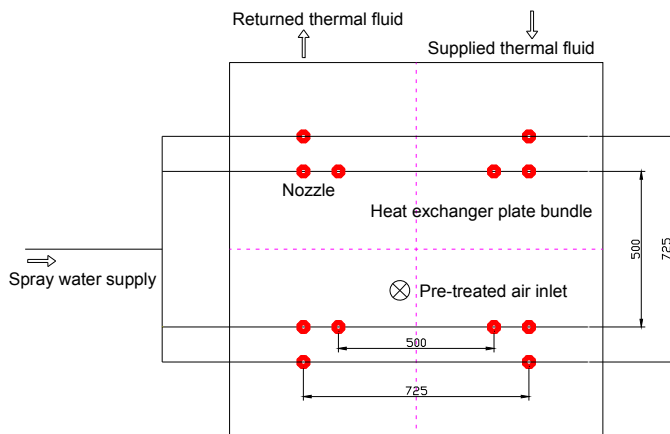


Figure 1: Corrugated plate spray humidification air-cooler



Figure 2: Experimental section of the corrugated plate heat exchanger



Figure 3: TF4 and AM4 nozzles

3. Comparison of Spray Cooling Effect

This section compares the cooling effects of the same nozzle type in different layouts to determine the optimal layout, and contrasts the cooling effects of different nozzle types in the same layout to identify the nozzle for optimal humidification.

3.1 The same nozzle type in different layouts

Based on previous research, three types of layouts were selected to determine the optimal layout, namely, 500mm×725mm, 500mm×500mm and 725mm×725mm.

The air cooling effects of the three layouts are compared in Figure 4, where the wet-bulb depression of inlet air is the cooling limit, and the spray amount is closely related to contact area between water vapour and the air. The air cooling effect was enhanced with the increase in the product of wet-bulb depression and spray

amount. The 500mm×500mm layout yielded the best cooling effect, followed in descending order by 725mm×725mm and 500mm×725mm. Hence, 500mm×500mm is the best layout in terms of air cooling effect.

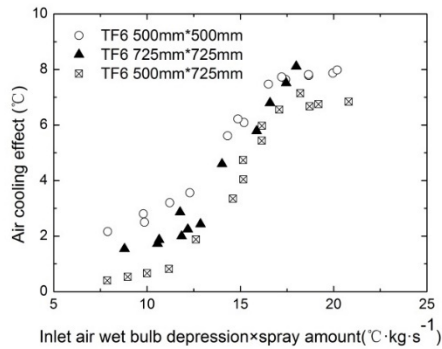


Figure 4: Air cooling effects of different layouts

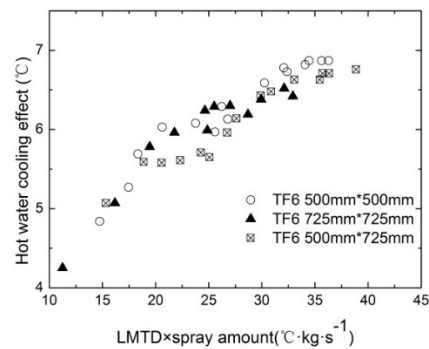


Figure 5: Water cooling effects of different layouts

The water cooling effects of the three layouts are compared in Figure 5, where the heat transfer is driven by the logarithmic mean temperature difference (LMTD). The water cooling effect was enhanced with the increase in the product of the LMTD and spray amount. The 500mm×500mm layout yielded the best cooling effect, followed in descending order by 725mm×725mm and 500mm×725mm. Hence, 500mm×500mm is also the best layout in terms of water cooling effect.

The experiment results show that 500mm×500mm is superior to 725mm×725mm and 500mm×725mm in both air cooling effect and water cooling effect.

3.2 Different nozzle types in the same layout

To determine the optimal nozzle for humidification, this section adopts the 500mm×500mm layout according to the experimental results in Section 3.1, and select the nozzle types of TF6×4 (two rows, each containing 2 nozzles) AM4×4, and TF6×2+AM4×2.

The air cooling effects of different nozzle types are compared in Figure 6. It can be seen that the air cooling effect was enhanced with the increase in the product of wet-bulb depression and spray amount. The TF6×4 boasts the best cooling effect, followed in descending order by AM4×4 and TF6×2+AM4×2. Hence, TF6×4 is the best nozzle type in terms of air cooling effect.

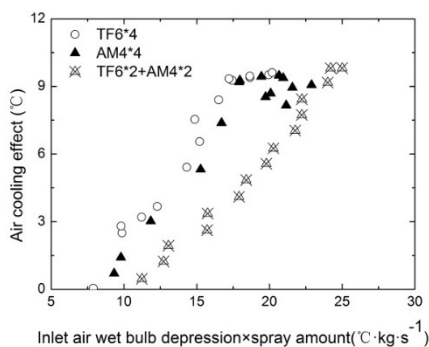


Figure 6: Air cooling effects of the different nozzle types

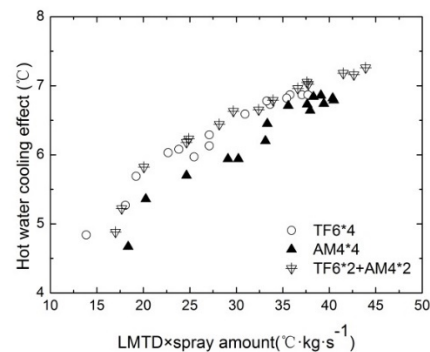


Figure 7: Water cooling effects of different nozzle types

The water cooling effects of different nozzle types are compared in Figure 7. As shown in the figure, the water cooling effect was enhanced with the increase in the product of the LMTD and spray amount. TF6×4 and TF6×2+AM4×2 exhibited better cooling effect than AM4×4.

The experimental results show that TF6×4 outperforms AM4×4 and TF6×2+AM4×2 in both air cooling effect and water cooling effect.

To sum up, the TF6 nozzle type + 500mm×500mm layout was confirmed as the optimal working conditions for the heat exchanger under wet conditions.

4. Air-Side Flow Resistance and Heat Transfer Features under Wet Conditions

Under wet conditions, the flow resistance drop on the air side of the air cooler increased with the face velocity (Figure 8). Based on the experimental data, the relationship between the air-side resistance drop, face velocity and plate width can be obtained as follows:

$$\begin{aligned} \Delta P_a &= 97.98 \times H \times v_a^2 \\ 0.3 \text{ m/s} &\leq v_a \leq 5 \text{ m/s} \\ R^2 &= 0.99619 \end{aligned} \quad (1)$$

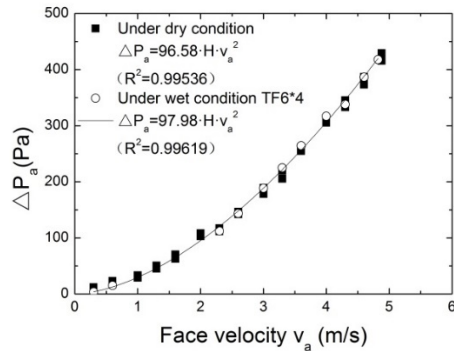


Figure 8: Air-side flow resistance drop curve

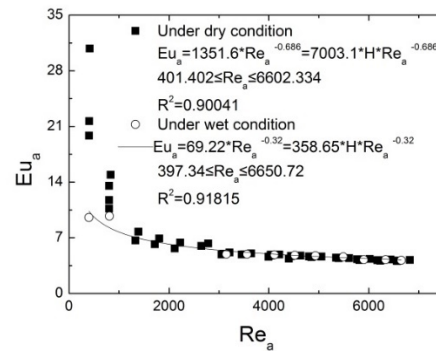


Figure 9: Relationship between Re_a and Eu_a

The sufficient turbulence was achieved when face velocity reached 3m/s. Based on the experimental data, the following expressions can be obtained:

$$\begin{aligned} Eu_a &= 358.65 \times H \times Re_a^{-0.32} \\ 397.34 &\leq Re_a \leq 6650.72 \\ R^2 &= 0.91815 \end{aligned} \quad (2)$$

Figures 8 and 9 show that the resistance drop curves and the resistance curves under wet conditions coincide with those under dry conditions. This means the unevaporated droplets did not obstruct the air-side flow, resulting in no reduction of air flow area or increase in air resistance.

Figure 10 depicts the relationship between the air-side Nu_a and the air-side Re_a . Under wet conditions, the relationship between Nu_a and Re_a on the air side can be obtained as follows:

$$\begin{aligned} Nu_a &= 0.032 \times Re_a^{1.140} \\ 397.34 &\leq Re_a \leq 6650.72 \\ R^2 &= 0.96852 \end{aligned} \quad (3)$$

According to Figure 10, as long as the air flow volume remains constant, the air-side heat transfer coefficient under wet conditions was much greater than it was under dry conditions; the heat transfer coefficient was 8~10 times as much as that under dry conditions at the moment of sufficient turbulence, and 8~16 times as much as that under dry conditions before that moment. The results indicate that the spray lowered the dry-bulb temperature of inlet air, and pushed up the LMTD over the corrugated plate, but the air-side heat transfer coefficient was increased as unevaporated droplets carried on with the heat absorption inside the plate.

5. Air-Side Mass-transfer Features under Wet Conditions

The spray cooling effect can be influenced by various factors, including but not limited to air mass velocity, nozzle type, distribution density, tube diameter, water pressure, as well as the contact duration, movement direction and initial/final parameters of the air and water. In typical air treatment processes, the most important factors are air mass velocity, water-air ratio and nozzle structure.

To depict the similarity between the actual process and the ideal process with limited water but sufficient contact duration, the contact coefficient η was introduced below:

$$\eta = 1 - \frac{t_2 - t_{s1}}{t_1 - t_{s1}} \quad (4)$$

where t_1 is the dry-bulb temperature of inlet air (□); t_{s1} is the wet-bulb temperature of inlet air (□); t_2 is dry-bulb temperature of outlet air (□).

Instead of mathematical calculation, the contact coefficient can only be determined through experiments. In the case of the same nozzle type in different layouts, the contact coefficient can be calculated by the following equation:

$$\eta = A(v\rho)^{m'}\mu^{n'} \quad (5)$$

where $v\rho$ is the air mass velocity ($\text{kg}/(\text{m}^2\cdot\text{s})$); v is the air velocity (m/s); ρ is the air density (kg/m^3); μ is the water-air ratio. The coefficient A and indices m' and n' can be acquired through experimental data fitting.

The spray water flow is generally expressed with the water-air ratio μ , that is, the water flow consumed in the treatment per kilogram of air:

$$\mu = \frac{W}{G} \text{kg}(\text{water})/\text{kg}(\text{air}) \quad (6)$$

where W is the aggregate spray water flow (kg/s); G is the air flow through the corrugated plate (kg/s).

The experimental data are sorted based on Equation (5). As shown in Figure 11, the contact coefficient increased with the water-air ratio when the air mass velocity reached $v\rho=3.6 \text{ kg}/(\text{m}^2\cdot\text{s})$. In other words, with the increase in water pressure, the dry-bulb temperature declined steadily before the air entered the corrugated plate. According to the experimental results, the contact coefficient was approximately 1, i.e. the cooling limit, at the air flow of $15,552 \text{ m}^3/\text{h}$ and the TF6×4 water pressure of 0.55 MPa . (Under the cooling limit, dry-bulb temperature drops to the wet-bulb temperature of inlet air. There is an optimal water pressure despite the simultaneous increase in water pressure and contact coefficient.)

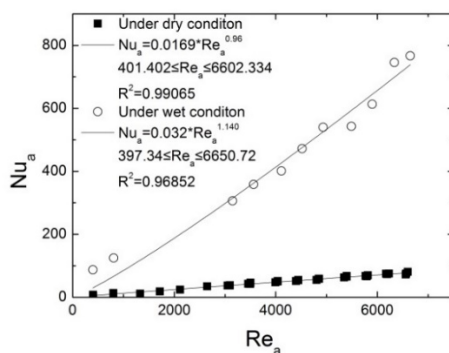


Figure 10: Relationship between the air-side Nu_a and the air-side Re_a

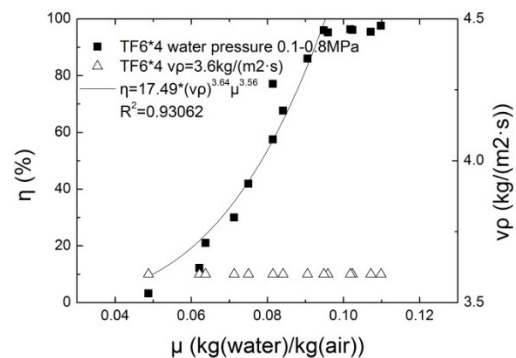


Figure 11: Variation in contact coefficient with the water-air ratio of TF6×4

6. Conclusions

(1) Through experimental data fitting, the author obtained the flow resistance and heat-transfer features on both the air side and fluid side under dry conditions, laying a solid basis for the design of corrugated plate air coolers.

(2) The TF6 nozzle type + $500\text{mm}\times 500\text{mm}$ layout was confirmed as the optimal working conditions for the heat exchanger under wet conditions.

(3) The spray lowered the dry-bulb temperature of inlet air, and pushed up the LMTD over the corrugated plate, but the air-side heat transfer coefficient was increased as unevaporated droplets carried on with the heat absorption inside the plate. The unevaporated droplets did not obstruct the air-side flow, resulting in no reduction of air flow area or increase in air resistance.

(4) The relationship between contact coefficient, air mass velocity and water-air ratio was obtained by data fitting before water pressure reached 0.55 MPa .

Acknowledgement

This paper is made possible by the generous support from Nanjing Institute of Technology (Grant No. YKJ201406) and the National Natural Science Foundation of China (Grant No. 51408302).

References

- Armbruster R., Mitrovic J., 1998, Evaporative cooling of a falling water film on horizontal tubes. *Experimental Thermal and Fluid Science*, 18(3), 183-194, DOI: 10.1016/S0894-1777(98)10033-X
- Bell I.H., Groll E.A., Koenig H., 2011, Experimental analysis of the effects of particulate fouling on heat exchanger heat transfer and air-side pressure drop for a hybrid dry cooler, *Heat Transfer Engineering*, 32(3-4), 264-271, DOI: 10.1080/01457632.2010.495618
- Cherif A.S., Kassim M.A., Benhamou B., 2011, Experimental and numerical study of mixed convection heat and mass transfer in a vertical channel with film evaporation, *International Journal of Thermal Sciences*, 50(6), 942-953, DOI: 10.1016/j.ijthermalsci.2011.01.002
- Duan Z., Zhan C., Zhang X., Mustafa M., Zhao X., 1998, Indirect evaporative cooling: Past, present and future potentials, *Renewable & Sustainable Energy Reviews*, 16(9), 6823-6850, DOI: 10.1016/j.rser.2012.07.007
- Kachhwaha S.S., Dhar P.L., Kale S.R., 1998, Experimental studies and numerical simulation of evaporative cooling of air with a water spray-I, Horizontal counter flow, *International Journal of Heat and Mass Transfer*, 41(2), 465-474, DOI: 10.1016/S0017-9310(97)00133-6
- Kim M.H., Kim J.H., Choi A.S., Jeong J.W., 2011, Experimental study on the heat exchange effectiveness of a dry coil indirect evaporation cooler under various operating conditions, *Energy*, 36(11), 6479-6489, DOI: 10.1016/j.energy.2011.09.018
- Stoitchkov N.J., Dimitrov G.I., 1998, Effectiveness of crossflow plate heat exchanger for indirect evaporative cooling: Efficacité des échangeurs thermiques à plaques, à courants croisés pour refroidissement indirect évaporatif. *International Journal of Refrigeration*, 21(6), 463-471, DOI: 10.1016/S0140-7007(98)00004-8
- Wang H.C., Mamishev A.V., 2012, Heat transfer correlation models for electrospray evaporative cooling chambers of different geometry types, *Applied Thermal Engineering*, 40(40), 91-101, DOI: 10.1016/j.applthermaleng.2012.01.061
- Xuan Y.M., Xiao F., Niu X.F., Huang X., Wang S.W., 2007, Research and application of evaporative cooling in China: A review (I)-Research, *Renewable & Sustainable Energy Reviews*, 16(5), 3535-3546, DOI: 10.1016/j.rser.2012.01.052
- Yan W., 1998, Evaporative cooling of liquid film in turbulent mixed convection channel flows, *International Journal of Heat and Mass Transfer*, 41(23), 3719-3729, DOI: 10.1016/S0017-9310(98)00105-7